Enzymatic monolithic reactors for micropollutants degradation

S. Ahmad, W. Sebai, M-P. Belleville, Nicolas Brun, A. Galarneau, José Sanchez-Marcano

Enzymatic Monolithic Reactors for Micropollutants Degradation

S. Ahmad[1], W. Sebai[1,2], M-P. Belleville[1], N. Brun[2], A. Galarneau[2], J. Sanchez-Marcano[1]

1 : Institut Européen des Membranes, UMR 5635, Université de Montpellier, CC 047, Place Bataillon, 34095 Montpellier cedex 5, France.

2: Institut Charles Gerhardt Montpellier, UMR 5253 CNRS – Université de Montpellier – ENSCM, 240 Avenue Emile Jeanbrau, 34296 Montpellier cedex 5, France.

Abstract

Silica monoliths with uniform macro-/mesoporous structures (20 µm and 20 nm macro- and mesopores diameters, respectively), high porosity (83%) and high surface area (370 m^2 g^{-1}) were prepared. The monoliths were grafted with amino groups (0.9 mmol NH_2 g^{-1}) and used to immobilize laccase from *Trametes versicolor* by covalent grafting with glutaraldehyde (GLU) (1.0 mmol GLU g^{-1}) leading to an ABTS activity of 20 U g^{-1}. Immobilization yield was 80%, based on the difference of initial and final activity of enzymatic solution used for immobilization. Enzymatic monoliths were used for the degradation of tetracycline (TC) in aqueous solution (20 mg L^{-1}) in continuous flow with recycling configuration. TC degradation efficiency was found to be 40-50 % after 5 h of reaction at pH 7. Enzymatic monoliths were used during 75 hours of sequential operation without losing activity. A Steady-state computational fluid dynamics (CFD) model based on Michaelis Menten reaction kinetics, allowed computing TC degradation efficiency.

Keywords: *enzymatic flow through reactor, monolith, laccase, antibiotic degradation, modeling, water treatment.*

1. Introduction

Antibiotics are commonly used in human and animal medicine for controlling and treatment of infectious diseases. A considerable amount of antibiotics is not metabolized in human or animal body and is thus discharged in wastewater and ends up in rivers, lakes and landfills. Antibiotics are refractory micropollutants, their concentration in treated wastewaters depends on their origin (domestic, hospitals or industrial), it is ranged from 10 ng L^{-1} to 10 µg L^{-1} [1]. Antibiotics, like tetracycline (TC) and oxytetracycline (OTC), are anti-microbial agents recalcitrant in nature; they are currently found in wastewaters and natural water bodies [2]. It has been found that TC and OTC increase the ecotoxicity and anti-microbial resistance [3], thus their presence in water can cause threat to human health.

Many pharmaceuticals present in wastewaters are not completely removed by conventional treatment plants [4, 5] and hence alternate removal techniques needs to be developed for the complete and efficient removal of these products. Biodegradation of antibiotics is recently been explored using oxidoreductases enzymes as a bio-catalyst [5].

Laccases are able to catalyze the oxidation of various aromatic compounds (particularly phenols) with the concomitant reduction of oxygen to water Their active site consists of 4 copper atoms, one responsible for the oxidation of phenolic groups and a cluster of 3 copper atoms responsible for the activation of oxygen. However, the mechanism of action of laccases, and in particular the role of the metal center, remains poorly known but many authors agree with the fact that it is a radical mechanism [6-9] (Figure 1). Laccase (EC 1.10.3.2) from *Trametes versicolor*, is an oxidoreductase enzyme which had been extensively studied for the biodegradation of antibiotics and found very promising due to its ability to oxidize large variety of these pharmaceuticals.

Nevertheless, generally enzymatic processes present some drawbacks like inactivation, lack of stability and reusability of enzymes, which can make the process uneconomical and unfeasible to be implemented on “large scale”.

Immobilization of enzymes improves the reusability and sustainability of enzymatic process [7] and allows bioreactors operating in continuous mode. Immobilization may improve

many enzymes properties like activity, stability, selectivity, specificity, inhibition [8-11]. Different Immobilization techniques have been used with different support materials [12], they include adsorption [13], encapsulation [14-16], covalent grafting [17], and adsorption followed by crosslinking [18]. The best method for biomolecules immobilization is not universal and will depend on the biomolecule itself. For laccases it was shown that a covalent grafting via a cross-linking agent such as glutaraldehyde is very efficient. Immobilization support materials like ceramic mono or multichannel membranes [19, 20], nano-fibrous membranes [21], metal nano-particles [22], carbon nanotubes [23] and mesoporous materials [24], magnetic cross-linked enzyme aggregates (M-CLEAs) [25] have successfully demonstrated the immobilization of laccase for the degradation of antibiotics. However, many of these materials present a limited surface area available for grafting; this is especially the case of membranes. Indeed, enzyme immobilization yields and reactivity are relatively low [26, 27].

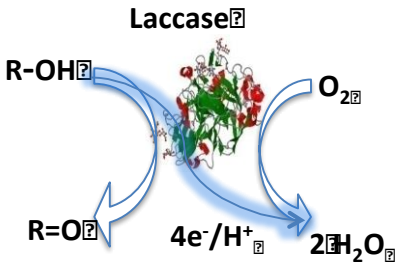

Figure. 1 General reaction mechanism of laccases.

Silica monoliths prepared by a combination of spinodal decomposition and sol-gel process have a homogeneous structure of macropores interconnected with mesopores in the skeleton. Macropores diameters are adjustable between 1 to 30 μm and mesopores diameters are adjustable between 8 to 20 nm leading to surface areas of 700 to 300 $m^2 g^{-1}$ and a total porosity around 85% [28]. These monoliths are able to allow large water flows to transfer through their structure with low pressure drop due to their homogeneous network of large communicating macropores. Enzymatic monoliths are interesting candidates to be applied in continuous flow through plug reactors. In this operating mode, the flow is forced to pass exclusively through the monolith porosity where the biocatalyst is immobilized and the contact between the reactants and the enzyme occurs during the mass transfer process. This configuration results in better control of the

reaction through the “micro-reactor concept”, where the distance between the biocatalyst and the substrate is considerably reduced, which increases the probability of reaction [29]. Moreover, monoliths have been successfully applied as a support material in chromatography [30], catalysis [31, 32] and for enzyme immobilization [33]. All these studies concluded that these structures are very promising as a solid support to immobilize catalysts due to their highly interconnected and homogeneous porous structure with large surface area available for grafting. Therefore, the aim of this research study was to immobilize laccase on silica monoliths to further explore the applicability of enzymatic monoliths for the degradation of TC, an antibiotic chosen as a model substrate. In this research work, silica monoliths were prepared with uniform macropores of 20 μm and mesopores of 20 nm diameters, and grafted with a commercial laccase from *Trametes versicolor* (kinetic diameter 6 nm, with four cupper atoms as metallic active center and an isoelectric point around 4.5). Covalent binding through glutaraldehyde was chosen as immobilization method since it has been successfully used to grafted laccase on ceramic membranes [19, 20]. Enzymatic monoliths were then used as a plug flow reactor operating in recycling-mode for TC degradation. Finally, a model was built by coupling the hydrodynamics with the experimental reaction kinetics using computational fluid dynamics (CFD) in order to optimize and simulate the process of degradation.

2. Materials and methods

Polyethylene glycol (PEG) (99%, 100 kDa), tetraethoxysilane (TEOS) (99%), (3-aminopropyl) triethoxysilane (APTES) (99%), commercial powder of laccase from *Trametes versicolor* (activity ≥0.5 U mg^{-1}), tetracycline (TC) (≥98.0%), glutaraldehyde (25% v/v) and 2,2'-azino-bis(3-ethylbenzothiazoline-6-sulphonic acid) (ABTS) (≥98.0%,) were purchased from Sigma-Aldrich.

2.1 Silica monoliths synthesis, functionalization and characterization.

Silica monoliths with hierarchical porosity (macro-/mesoporosity) were prepared by a controlled sol-gel process with TEOS and PEG according to a method previously reported [28]. The surface area of silica monolith before enzyme immobilization was 336 m^2 g^{-1}. Prior to enzyme immobilization, the monoliths were pre-activated by grafting amino groups. For this purpose, they were firstly dried at 250°C under vacuum for 4 h and then immersed in a solution of APTES

in ethanol (in order to have an excess of 10 amino groups per nm^2). The activation was carried out under reflux (80 °C) overnight. The reactors were built by cladding the monoliths inside Teflon™ heat shrinkable gains at 180 °C for 2 h to be finally connected to stainless-steel tubing. This tubular plug-flow reactor configuration allowed the liquid feed penetrating the internal porosity of activated monoliths without preferential ways.

The monoliths were named as "preactivated monoliths" before enzyme grafting and "laccase-activated" or "enzymatic monoliths" after enzyme immobilization, for instance see section 2.3. Monoliths were characterized structurally by scanning electron microscopy (SEM) (Hitachi S-4800 I FEG-SEM). Porosity was determined by mercury porosimetry (Micrometrics Autopore 9220) and nitrogen adsorption at 77 K (Micromeritics Tristar 3020). Before nitrogen adsorption measurements, monoliths were outgazed for 12h at 250°C and 80°C for raw and grafted silica monoliths respectively. The quantitative determination of the number of amine functions on the surface of the silica monolith was determined by TGA analysis (PerkinElmer STA 6000) using a high resolution program (from 40 to 900 °C) under air with a ramp of 10°C per minute. The number of grafted functions was determined by the loss of weight of the material from 200°C to 900°C and taking in account the dehydroxylation of the surface of the monolith.

2.2 Permeability tests

Permeability tests were carried out both before and after immobilization of enzymes by filtrating osmosed water through the monoliths. Monoliths of 0.6 cm diameter and 0.5 cm length were connected to a flow system consisting of a HPLC pump and a pressure gauge as shown in Figure 1. The flow rates were varied from 1 mL min^{-1} to 5 mL min^{-1}. The back pressure exerted by monoliths was measured thanks to a pressure gauge and then permeability (k) was calculated by Darcy equation as follows:

$$k = \frac{Q}{A}\frac{l}{\Delta P}\mu \qquad (1)$$

With k Permeability coefficient (m^2), Q the flow rate (m^3s^{-1}), A the cross section of the monolith (m^2), μ the viscosity of the fluid (μ = 1.002 mPas at 20 °C for water), l the length of the monolith (m) and ΔP the difference of pressure at the outlet and inlet of the monolith (Pa).

2.3 Laccase immobilization

Covalent immobilization of enzymes through glutaraldehyde binding is a widely used immobilization method that prevents enzyme leakage. Moreover, previous works confirmed that this method can be successfully used to grafted this commercial laccase on ceramic membranes [19,20]. Laccase immobilization was carried out by putting into contact the preactivated monoliths within a glutaraldehyde solution 4 % (v/v) prepared in a citrate phosphate buffer solution (pH 7, 0.1 M). For this purpose cladded monoliths were filled with 0.5 mL of glutaraldehyde solution and allowed to react for 30 minutes. Monoliths were then rinsed 5 times with 0.5 mL of the same buffer solution in order to remove unreacted glutaraldehyde. During the reaction between glutaraldehyde and APTES the white or pale yellow monoliths turn deep orange within minutes. This change in colour indicates that the reaction has occurred and has been explained by George et al [34] as the result of the formation of an aldimine (Schiff linkage (=CHN=), between the free amino groups of APTES and glutaraldehyde.

Finally, monoliths were filled a volume of laccase solution (5±1 U mL_{sol}^{-1}) prepared in a citrate phosphate buffer (pH 7, 0.1 M). For this purpose the enzymatic solution was introduced at the entrance of the tube containing the monolith, allowing the penetration into the monolith porosity by capillarity. The tube was closed and turned several times during 1 hour, and then rinsed with the buffer solution. After immobilization, enzymatic monoliths were stored in the same buffer solution at 4°C. It is worth noting that grafted monoliths were stable under washings and tests, thus it can be assumed that enzymes were covalently immobilized.

The schematics of covalent bonding through the monolith and APTES and formation of aldimine are illustrated in Figure 2.

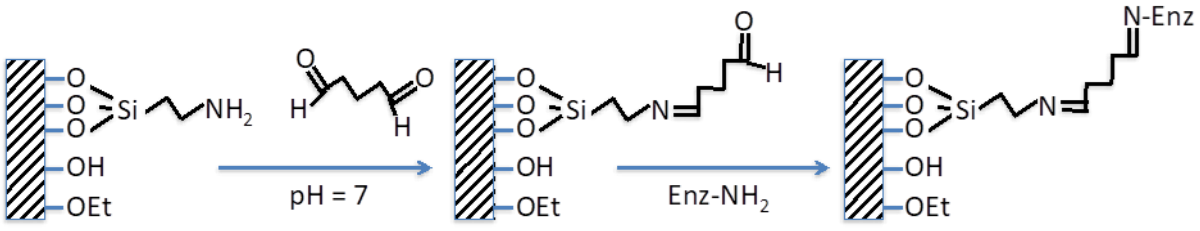

Figure 2. Schematic of enzyme covalent bonding through APTES loaded monoliths

2.4 Activity measurement

Activity (U mL^{-1}) of free laccase was measured using 2,2′-Azinobis-(3-ethylbenzthiazoline-6-sulphonate) (ABTS) as substrate. 100 µL of diluted enzyme solution was added to 900 µL of 1 mM ABTS solution prepared in a citrate phosphate buffer solution (pH 4, 0.1 M), absorbance change was followed for 1 minute by spectrophotometry at 420 nm (ε = 3600 $M^{-1}cm^{-1}$), activity (U mL^{-1}) was then estimated by slope of absorbance vs time.

The measurement of the enzymatic activity of immobilized laccase was carried out with crushed laccase-activated monoliths; 5 mg of the active powder were added to 25 mL of ABTS solution (1 mM) prepared in the same citrate phosphate buffer mentioned above in a 100 mL flask at 25°C, under air and agitation. The activity (U $mg_{monolith}^{-1}$) was estimated as explained above by the change in absorbance of the ABTS solution.

The enzyme immobilization yield was calculated considering the activity of the enzyme stock solution used for immobilization before and after activation process taking into account the activity of rising solutions as expressed in Equation 2 and 3.

$$A_{immobilized} = A_{initial} - (A_{left} + \sum A_{rinsing}) \quad (2)$$

$$\rho_{immobilization} = \frac{A_{immobilized}}{A_{initial}} \times 100 \quad (3)$$

2.5 Determination of reaction kinetics parameters for free and immobilized laccase

Apparent reaction kinetic parameters for free and immobilized laccase (with crushed monoliths) were determined using ABTS and TC as substrates. For this purpose an equivalent amount of 0.01U of enzyme (liquid solution of enzyme or crushed laccase-activated monolith) were added to 25 mL of ABTS solution (20 - 100 µM in citrate phosphate buffer solution, pH 4). In the case of experiments with TC the amount of free (5.0 U) and immobilized enzyme (3.0 U) were added to 10 mL of TC solution (2 - 20 ppm in osmosed water, pH 6). Runs for both substrates were carried out in stirred Erlenmeyer flasks under air atmosphere. Linear regression was applied on the obtained data and then apparent reaction kinetic parameters (V_{max} and K_M) were determined by Lineweaver-Burke plot according to equation 4:

$$\frac{1}{V} = \frac{K_M}{V_{max}} \frac{1}{[S]} + \frac{1}{V_{max}} \quad (4)$$

Here V is the rate of substrate consumption (µmols^{-1}); V_{max} is the maximum rate of substrate consumption (µmols^{-1}) and K_M is the Michaelis-Menten constant (µmol) and S the substrate concentration (µmol).

2.6 Tetracycline degradation tests

TC degradation tests were carried out with three laccase-activated monoliths connected in series (0.6 cm diameter and 0.5 cm length, each, equivalent to a total of 15.0 U ± 1.5 U of enzymatic activity). The recirculation of the flow was ensured by a HPLC pump (Gibson model: 321, France) as shown in Figure 3. A pressure sensor was connected at inlet of monoliths to measure back pressure. TC solution (20 ppm) prepared in osmosed water pH 6, at 25°C was flowed through the enzymatic monoliths in continuous recycle-mode. The flow rate was kept at 1 mL min^{-1}. Samples were taken from the reservoir and analyzed by high-performance liquid chromatography coupled to triple-quadrupole mass spectrometry (HPLC–MS). Samples were injected through a Macherey-Nagel C18 column (50 mm x 2 mm) with a Waters e2695 Separations Module, and the 410 m/z fragment was detected with a Micromass Quattro micro API device.

2.7 Storage and operational stability of laccase-activated monoliths

The stability of enzymatic monoliths under storage conditions (citrate phosphate buffer (pH 7) at 4 °C was determined by measuring the residual activity over a 30-day period. For this purpose several enzymatic monoliths (10) were prepared under the same conditions, then they were stored and every 5 days samples were taken and their activity measured according to the protocol explained in section 2.4. The stability of laccase-activated monoliths under continuous operation was also studied for TC degradation. For this purpose TC (20 ppm) degradation tests were carried out following a sequential procedure: after 8 hours of reaction the pilot was emptied, rinsed with osmosed water and kept at room temperature overnight, then a new fresh TC solution was introduced and the run start again. The cycles were repeated for a total duration of 75 hours.

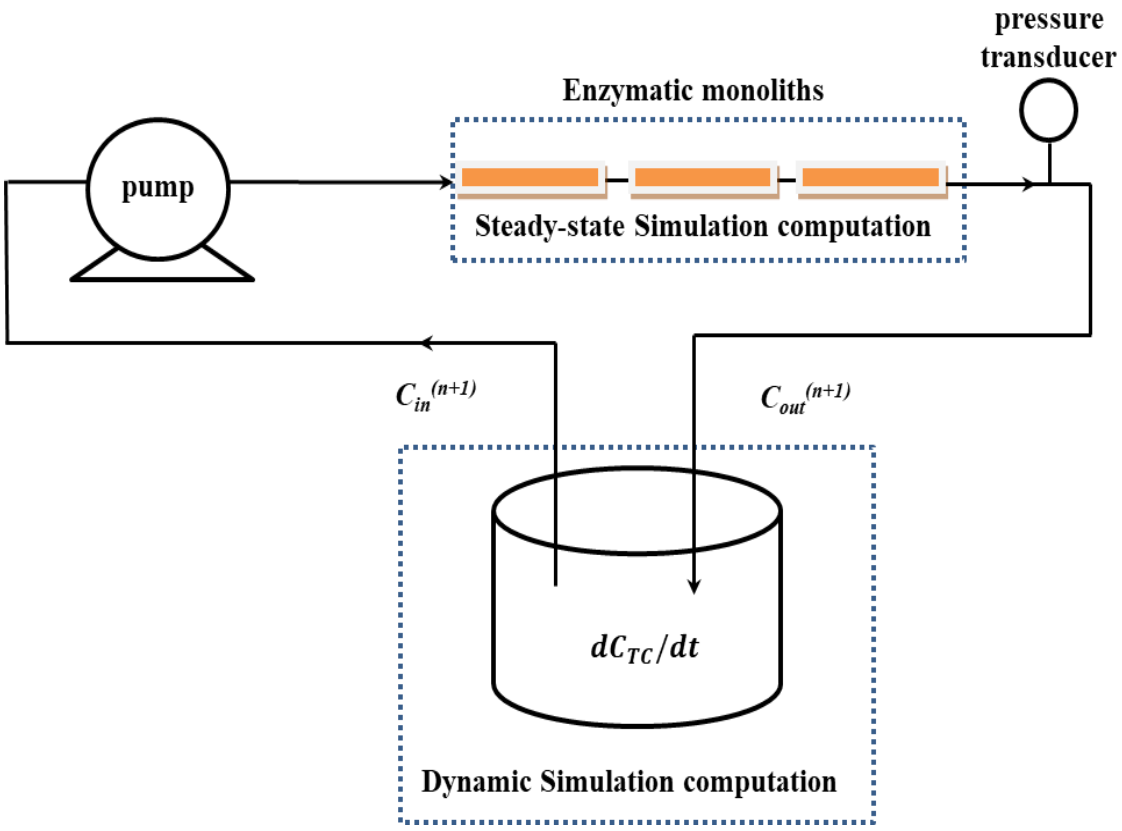

Figure 3. Schematic draw of pilot for TC degradation with recycling.

3. Modeling and Simulation

To setup the "steady-state model" a homogenous porous structure was considered, keeping in view a global porosity and permeability through all monolith volume. A Steady state modeling was based on the coupling of mass balances, hydrodynamics inside the monoliths' porosity and enzymatic kinetics [35]. Permeability and reaction kinetics parameters (K_M and V_{max}) used in modeling were measured experimentally as discussed in section 2.5. From the results of steady-state modeling, TC concentration evolution along the length of reactor was computed. Dynamic model was setup by taking mass transfer balance on the feed tank considering monolith as a plug-flow reactor. The concentration field (C) for TC was calculated from the mass balance and reaction rate taking into account the TC depletion. As far as the reaction extend was based on the reactant consumption for the modeling, the classical mass balance equation coupling diffusion, convective flow and reaction kinetics was be employed:

$$\nabla(-D_i \nabla c_i) + u \nabla c_i = Ri \quad (5)$$

Eq. 5 is the basic mass transport equation which couples the reaction rate with the flow within the monolith geometry, it is applied to simulate the concentration gradient (∇c_i) along the length of the monolith geometry. It includes TC diffusion coefficient (*Di*), velocity within porous domain (*u*), and enzymatic reaction rate (*Ri*). Velocity was calculated within geometry by applying Brinkman equation (Eq. 6) which is used to describe flowing fluids though porous materials under laminar conditions [36–38]. Indeed the Re value calculated for the flow conditions in this study (i.e. 2) was less than 10 allowing the use of Brinkman equation.

$$\nabla \left[-PI + \mu \frac{1}{\varepsilon_p} (\nabla u + (\nabla u)^T) - \frac{2}{3} \mu \frac{1}{\varepsilon_p} (\nabla . u) I \right] - \left(\mu k^{-1} + \beta_F |u| + \frac{Q_m}{\varepsilon_p^2} \right) u + F = 0 \quad (6)$$

where ε_p is the global porosity of the domain; k (m^2) is the permeability of the domain; u ($m\ s^{-1}$) is the Darcy's velocity (the ratio of flow rate to monolith cross section) and μ (mPa s) the viscosity of the solution.

Similarly reaction rate (Eq.7) was estimated by introducing Michaelis-Menten equation applied to the TC degradation in the model.

$$R_i = \frac{V_{max} C_i}{K_M + C_i} \quad (7)$$

where C_i is TC concentration.

The main assumptions taken for the model are:

- Isothermal operation.
- Global and homogeneous porosity through all monolith volume.
- Enzymatic activity and permeate flow rate are constant.
- Physical properties of reaction media (viscosity, density) are constant under different operating conditions.

Equations (5) to (7) were coupled and solved simultaneously with COMSOL Multiphysics® software (version 5.3). Physics controlled fluid dynamic fine size mesh was used. Maximum and

minimum element size was 0.06 and 0.32 mm. Further decreasing the element size had no effect on output TC concentration.

Dynamic modeling was then performed by applying mass transport balance in the reservoir and closed loop as explained by Younas et al. [39]. For this purpose Matlab® (version 18) was implemented to update the output results obtained from Comsol Multiphysics®. In order to couple the both software, live-link application was used.

Mass transport modeling in the reservoir

As far as the TC concentration in the tank decreased gradually the dynamic variation of TC concentration with time was calculated by applying a transient differential equation around the tank:

$$V\frac{dC_{TC}}{dt} = Q({C_{in}}^{n+1} - {C_{out}}^{n+1}) \quad (8)$$

4. Results and discussion

4.1 Structural characterization of monoliths

Nitrogen adsorption/desorption isotherms at 77 K and mercury porosimetry measurements shown that monoliths present a very high porous structure with a total porosity of $\varepsilon = 0.83$ (V_{macro} = 3.0 mL g^{-1}, V_{meso} = 0.8 mL g^{-1}), a low density of 0.20 g cm^{-3} and mesopores with a mean diameter of 18 nm developing a large surface area of 336 m^2 g^{-1}. The macroporous surface determined by mercury porosimetry is around 1 m^2 g^{-1}. After the activation, amino-functionalized monoliths contain 0.8 mmol NH_2 $g_{monolith}^{-1}$ corresponding to a grafting of 1.5 NH_2 per nm^2 with 72% of tridentate silanes (28% of bidentate). After laccase immobilization by covalent grafting through glutaraldehyde bounds important textural changes occur with a decrease of the specific surface area (164 m^2 g^{-1}), V_{meso} (0.5 mL g^{-1}) and mesopores diameter (15 nm). Figure 4 shows a SEM picture of the structure of a raw silica monolith (4a) and laccase-grafted monolith (3b). From Figure 4a we can notice the interconnected macropores network of approximately 20 μm of average diameter and a skeleton thickness of around 6 μm. The aspect of grafted monolith presents a slight difference respect to the raw one, only the softness of the surface seems to be

enhanced indicating the possibility of the formation of a thin film of immobilized enzyme on the surface. This effect is more marked in Figures 4c and 4d which show corresponding magnifications of Figure 4a and 4b respectively.

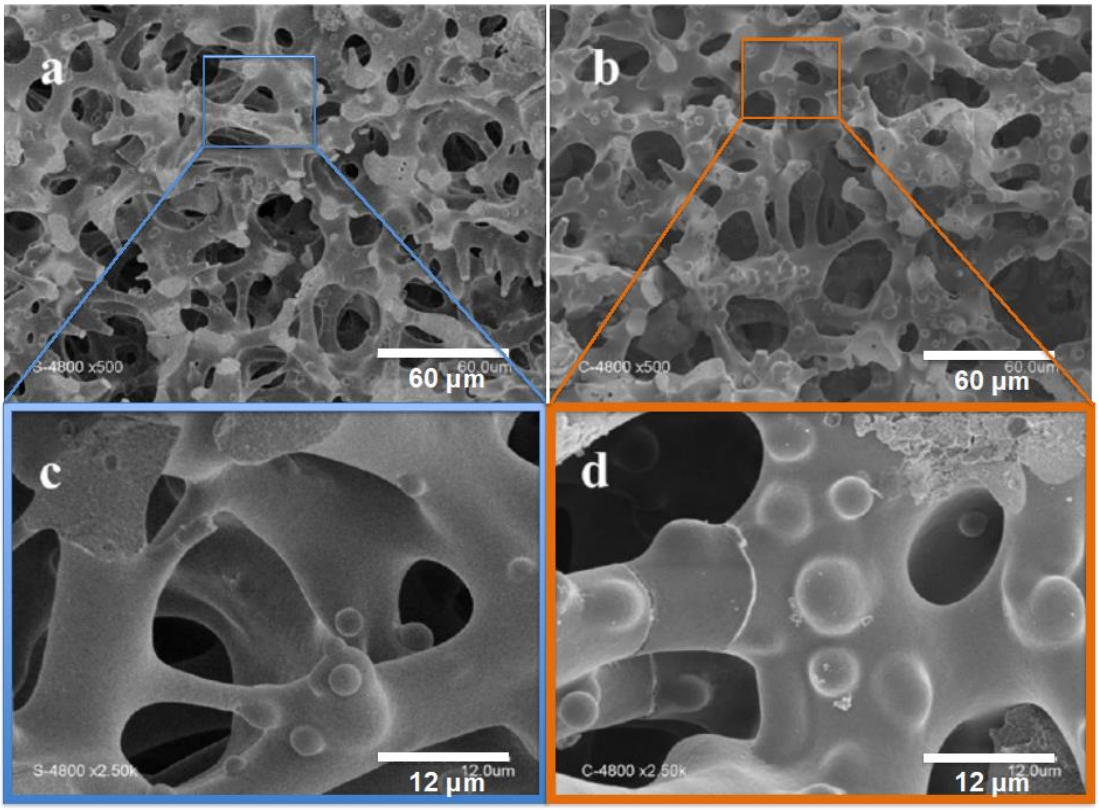

Figure 4. SEM of monoliths showing the macroporous structure. a) Raw monolith, b) Laccase-grafted monolith, c) and d) are respectively magnification figures a) and b).

Many hypotheses can be done to explain this behavior; on one hand laccase grafting was occurring more extensively in the mesoporosity, on the other hand a very thin layer of the immobilized enzyme was perhaps covering the internal surface of the surface of the solid (as is observed in Figures 4b and 4d above). The very thin coating does not significantly affect the macroporosity but it can partially cover mesopores' mouth. Moreover, the decrease of the specific surface, mesopores volume and diameter discussed above are also indications that both hypotheses are possible.

4.2 Permeability coefficient

When water flow rate varied from 1 to 4.5 mL min^{-1} through a cladded monolith, the upstream pressure increased linearly from 10 to 40 mbar. These measured values of upstream pressure are very low and confirm that monoliths present interesting structure with very high porosity and communicating macropores. Permeability coefficient (*k*) of raw silica monoliths calculated from Equation1 was equal to 5.9 10^{-12} m^2. Other authors has reported the same order of magnitude of permeability (11 10^{-12} m^2) [40] but with monoliths with pore size of 30 – 50 µm. After enzyme immobilization, no change was observed for the value of permeability coefficient; enzyme grafting does not affect the mass transfer.

4.3 Activity and immobilization yield

The activity of a single monolith (6 mm diameter and 5 mm length, mass of 50 mg) was determined using crushed monoliths as explained in section 2.4. The mean activity of enzymatic monoliths was of 5.0 ± 0.5 U. The immobilization yield of enzymes is an important factor for process efficiency and cost. Immobilization yield measured was equal to 80 ± 5%. This relatively high immobilization yield is certainly reached because the small volume of enzymatic solution employed together with the high specific surface with a high number of reactive sites (amino groups coupled with glutaraldehyde). The immobilization probably also favored by the structure of monoliths of extremely interconnected macroporous and mesoporous networks and the thin skeleton (6 µm), which reduces the diffusion path lengths facilitating the access to the numerous reactive sites. It is important to notice that grafted monoliths were stable under washings and after successive reactivity tests, thus it can be assumed that enzymes were covalently immobilized.

These initial results conclude a successful immobilization of laccase on silica monoliths and demonstrated very high immobilization yield.

4.4 Determination of apparent reaction kinetic parameters

Apparent kinetic parameters K_M and V_{max} for both free and immobilized enzymes (crushed monoliths) were determined with two different substrates ABTS and TC by the method discussed above in section 2.5. Measured values are shown in Table 1. It can be observed that after

immobilization the apparent K_M value decreased by 1.6 and 4 times for ABTS and TC, respectively. This result is surprising because generally structural conformation and diffusion limitations occur after immobilization. However, a similar trend has already been reported for laccase immobilized on membranes [19, 20] and lipase on mesoporous SiO_2 microparticles [41]. V_{max} value depends on the concentration of the enzymatic solution (for free enzymes) or the amount of immobilized enzymes on a support. In this work the kinetic experiments with ABTS were carried out in order to have in both cases, the same amount of enzymes in terms of activity towards ABTS (i.e. 0.25 U). It was observed that V_{max} value was higher for immobilized enzymes indicating a better reactivity of immobilized biocatalyst. As in the case of K_M, this result is in good agreement with previous results reported by De Cazes et al (2014) [19, 20]. For TC, since activity used for free and immobilized was not same (0.3 U mL^{-1}) and (0.15 U mL^{-1}), respectively, it was not possible to compare the V_{max}.

Table 1. Apparent reaction kinetic parameters for the oxidation of ABTS and tetracycline (TC) with free and immobilized laccase.

substrate	State of Enzymes	V_{max} (µmol min^{-1}) ±10%	K_M (µmol L^{-1}) ±10%
ABTS	Free	$1.3\ 10^{-2}$	85
	Immobilized	$6.4\ 10^{-2}$	50
TC	Free	$7.0\ 10^{-4}$	80
	Immobilized	$2.0\ 10^{-4}$	20

4.5 Tetracycline degradation tests

TC (20 ppm) degradation results are displayed in Figure 5. Control experiments (blank tests) were carried out to study the effect of TC self-degradation or adsorption on the evolution of TC concentration. For these tests, enzymatic monoliths were first thermally deactivated by heating in oven at 100°C for 2 hours. The results of control experiments show that less than 2% of initial TC was removed. The evolution of TC concentration with enzymatic monoliths shows that

laccase-activated monoliths were able to degrade 40% of initial TC in first 5 hours and then the degradation rate decreases dramatically. From this point the TC concentration decreases slowly up to 50% at 26 hours of reaction. Many hypotheses can be done to explain this behavior; they include the decrease of substrate concentration, if the kinetics obeys to a Michaelis-Menten equation. However, the diminution of the oxygen content, or even the formation of inhibiting by-products can also be considered.

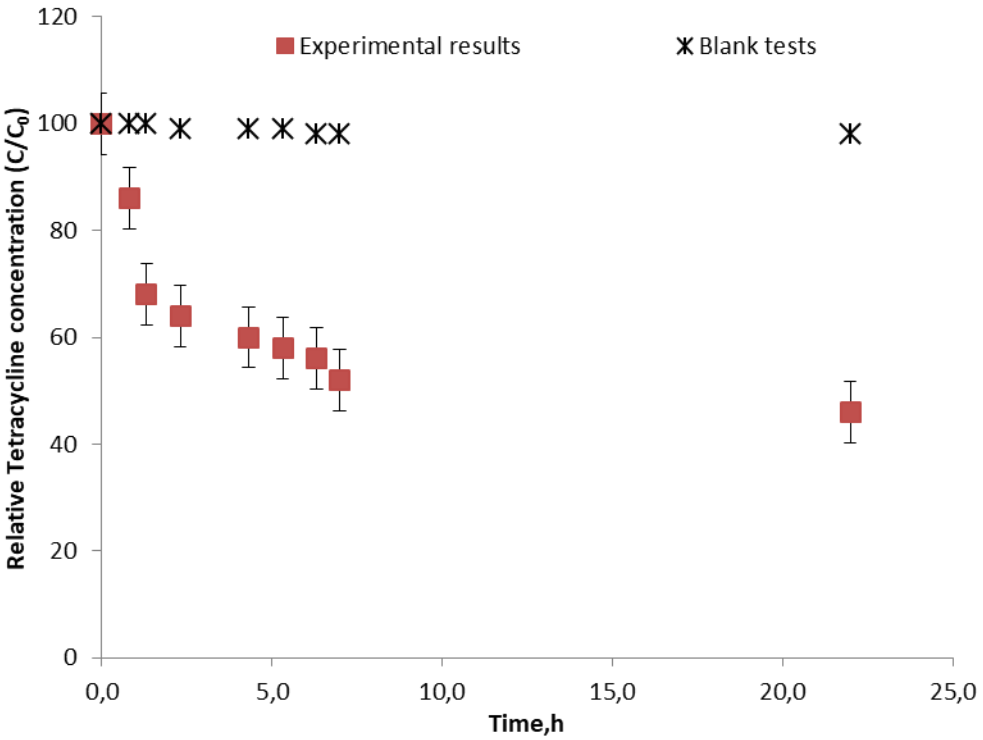

Figure 5. Degradation of TC. C/C_0: variation of the TC concentration respect to the initial TC concentration (20 ppm).

Some authors [29, 30] have noticed that the velocity of oxidation of substrates by laccases can decrease very rapidly during the first hours of reaction because the oxygen concentration depletion near catalytic sites. Indeed, the conversion can be improved by stirring on air atmosphere or reach 100% by using pure oxygen [30]. In the case of experiments carried out in the monolithic system in continuous configuration no stirring under air or oxygen was done. In addition, the concentration of enzyme was relatively high (15.0 U for 30 mL of 20 ppm of TC

solution) and even if the calculated total initial amount of oxygen ($7.7\ 10^{-7}$ mol) was 5.5 times the initial amount of TC ($1.4\ 10^{-7}$ mol) it is possible that the oxygen depletion near the catalytic sites caused the observed decrease of the degradation rate. This effect was already demonstrated in the literature [29, 30]. Moreover, TC degradation results in many different by-products that can also be oxidized by laccases [42, 43] (sometimes, first oxidation products are more reactive that the initial substrate). Indeed, the oxygen necessary for the degradation of TC can also be consumed by these side reactions. This point is certainly critical for the conversion reached with enzymatic reaction within the porosity of the monoliths. Additional experiments were carried out under the same conditions (volume and concentration of solution, amount of activated monoliths) of the continuous configuration but with crushed activated monoliths in a stirred batch reactor with air bubbling. The results showed a total TC depletion in 6 hours. Indeed, the hypothesis of inhibition by products formation can be omitted.

4.6 Storage and operational stability of laccase-activated monoliths

Storage and operational stability of immobilized laccase is an important step for its practical applicability and plays a key role in process cost. Storage stability was studied for 30 days as explained in section 2.7. The results obtained demonstrated that there was no loss of enzymatic activity during the first 5 days of storage at 4°C. Then during the other 25 days of storage the activity decreased slowly reaching approximately 85% of the initial one. Similarly, the activity of free enzymes was studied under same storage conditions and for same time period as immobilized enzyme. The results demonstrated that there was no noticeable change in the activity of free enzymes even after 30 days of storage at 4ºC.

The operational stability of enzymatic monoliths was studied during 75 hours with the cyclical procedure described in section 2.7; the results are displayed in Figure 4. We can observe that the evolution of TC concentration is very similar for all of the cycles. As it was discussed in section 4.5, TC concentration decreases very rapidly during the first minutes of operation and then the degradation rate slowdown. When the solution is changed with a fresh one containing the initial TC and oxygen concentration the same pattern of TC depletion is obtained. Indeed we can conclude that the enzyme immobilized in monoliths is stable during at least 75 hours of operation. The slowdown of the reaction rate could be avoided by using air or oxygen bubbling in

the reservoir.

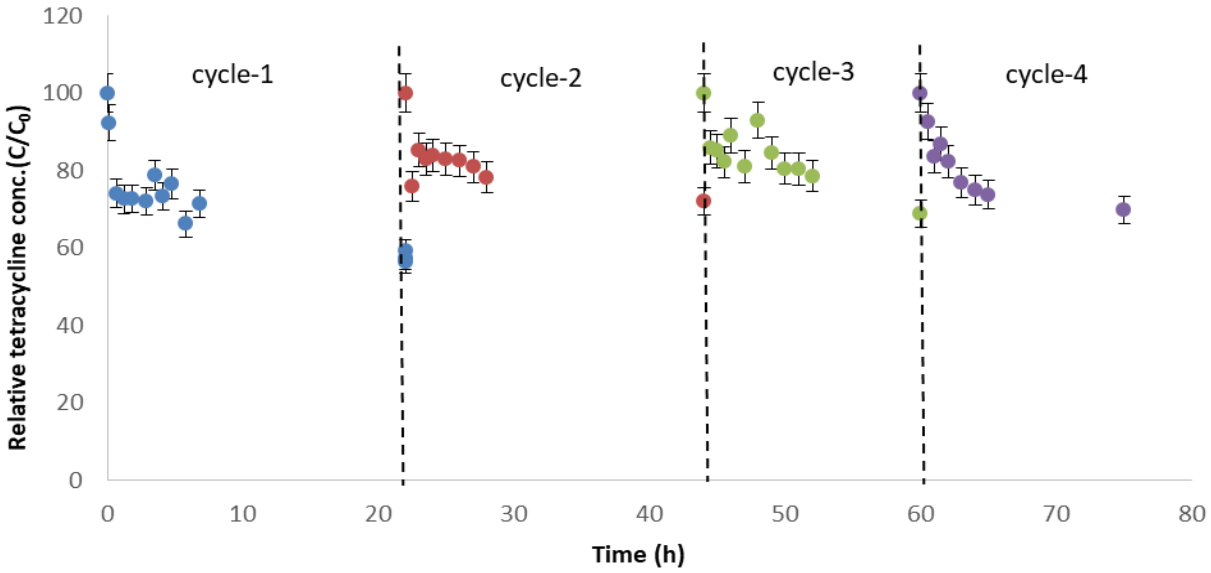

Figure 6: Operational stability of monoliths for 75 hours of sequential operation.

4.7 Simulation

As explained in section 3, the steady state model (Eq.5-7) was coupled with the dynamic mass (Eq.8) transfer applied on feed tank, using the outlet results from monolith and running a closed loop in Matlab®. Results of the dynamic mass balance simulation in the reservoir tank allowed calculating the degradation rates of substrate. The evolution of residual TC concentration is shown in Figure 5a. The results of the model simulate relatively well the experimental evolution of TC concentration in the tank during the first 5 hours, period in which we can consider that Michaelis-Menten kinetics is valid because we don't have deficiency of oxygen to carry out the degradation. Steady-state model was solved in COMSOL Multiphysics® considering the three monoliths in series as a single plug flow reactor. The output concentration for single pass (residence time for single pass 45-50 seconds) was calculated from surface integration at the outlet of monolith. Results are shown in Figure 5b. It can be seen that TC concentration decreases along the reactor's length, but the conversion is relatively low at each passage (0.02 µmol L^{-1}).

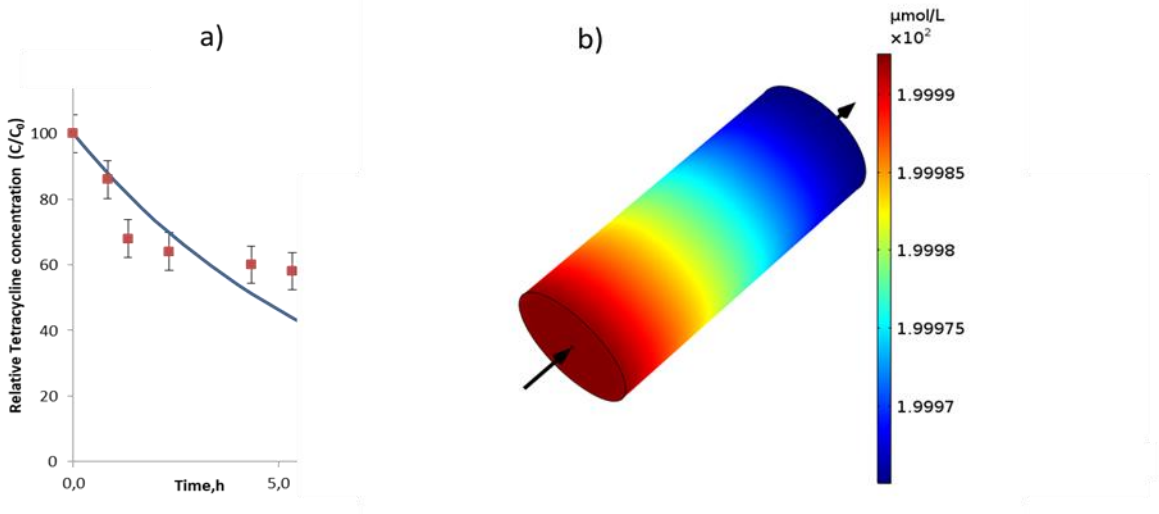

Figure 7. a) Evolution of TC concentration inside the reservoir. Comparison of experimental and modeling base results from a dynamic simulation, ■ experimental results, simulation. b) Steady state CFD simulation results showing TC concentration change along the length of the reactor for a single pass.

5 Conclusions

Silica monoliths with a homogenous mesoporous/macroporous structure featuring, high specific surface area and porosity were successfully prepared. These monoliths were preactivated with APTES and glutaraldehyde in order to covalently immobilize laccase from *Trametes versicolor*. From reaction kinetic parameters V_{max} and K_M values, it was concluded that after immobilization laccase was more active without losing affinity to substrate. Enzymatic monoliths were successfully implemented at laboratory scale for the degradation of tetracycline as model micropollutant in a continuous plug flow mode with recycling. System of three monoliths, connected in series was able to degrade 40-50% of TC in 20 ppm solutions in 5 hours. The immobilized laccase on silica monoliths exhibited high stability during storage as well as good operational stability during 75 hours of sequential operation both factors are interesting for their applicability at large scale.

Modelling and simulation of the TC concentration evolution for the plug flow reactor coupling the hydrodynamics and kinetics was in good agreement with experimental results for the first 5 hours of reaction. However, at longer times of reaction it was observed experimentally that the degradation rate slowdown, this behavior may be the result of a high enzymatic activity which causes a rapid lack of oxygen, co-substrate essential for the oxidation reaction. Indeed, the actual

configuration of the plug flow reactor doesn't allow a continuous aeration or feed of oxygen. In a future; the design and scale up the pilot unit will have to consider an aeration system in the reservoir or in between the monoliths and a continuous process without recycling. Moreover further experiments will be conducted in order to identify the parameters of a new kinetics considering tetracycline and oxygen concentration.

Acknowledgments

This research was funded by the ANR French agency, project MUSE ANR-16-IDEX-0006 project DEMEMO. Mr. S. Ahmad acknowledges the Higher Education Commission, Pakistan for the PhD scholarship. The authors wish to acknowledge the support from the chemistry plateform of campus in Montpellier (Plateform MEA University of Montpellier), where SEM has been performed.

Notations and symbols

Symbol	Defintion
A	Cross-sectional area (m^2)
$A_{immobilized}$	Activity immobilized ($U\ g^{-1}$)
$A_{initial}$	Activity of enzymatic solution before immobilization (U)
A_{left}	Activity of enzymatic solution after immobilization (U)
$A_{rinsing}$	Activity of the rinsing solution (U)
C_{in}^{n+1}	Inlet concentration for n+1 loop ($\mu mol\ L^{-1}$)
C_{out}^{n+1}	outlet concentration for n+1 loop ($\mu mol\ L^{-1}$)
C_{TC}	Tetracycline (TC) concentration ($\mu mol\ L^{-1}$)
D_i	Diffusion coefficient ($m^2\ s^{-1}$)
F	Volume Force (Nm^{-3})

I	Identity vector
k	Permeability coefficient (m^2)
K_M	Michaelis constant (µmol L^{-1})
l	Length of the monolith (m)
P	Pressure (Pa)
Q	Flow rate (mL min^{-1})
Q_m	Mass source term (kg $m^{-3}s^{-1}$)
R_i	Reaction rate (µmol m^{-3} s^{-1})
[S]	Substrate concentration (µmol L^{-1})
u	Darcy velocity (m s^{-1})
V	Reaction rate (µmolmin^{-1})
V_{max}	Maximum reaction rate (µmolmin^{-1})
μ	Fluid viscosity (mPa.s)
$\rho_{immobilization}$	Immobilization yield
∇c_i	Concentration gradient (µmol L^{-1} m^{-1})
ε_p	Porosity
β_F	Forchheimier coefficient (kg m^{-4})
$\sum$	Summation

References

[1] M.-C. Danner, A. Robertson, V. Behrends, J. Reiss, Antibiotic pollution in surface fresh waters: Occurrence and effects, Sci. Total Environ. 664 (2019) 793–804. https://doi.org/10.1016/j.scitotenv.2019.01.406.

[2] U. Szymańska, I. Soltyszewski, J. Kuzemko, G. Wiergowska, M. Woźniak, Presence of antibiotics in the aquatic environment in Europe and their analytical monitoring: Recent trends and perspectives, Microchem. J. 147 (2019) 729–740. https://doi.org/10.1016/j.microc.2019.04.003.

[3] B. Halling-Sørensen, G. Sengeløv, J. Tjørnelund, Toxicity of Tetracyclines and Tetracycline Degradation Products to Environmentally Relevant Bacteria, Including Selected Tetracycline-Resistant Bacteria, Arch. Environ. Contam. Toxicol. 42 (2002) 263–271. https://doi.org/10.1007/s00244-001-0017-2.
[4] P.E. Stackelberg, E.T. Furlong, M.T. Meyer, S.D. Zaugg, A.K. Henderson, D.B. Reissman, Persistence of pharmaceutical compounds and other organic wastewater contaminants in a conventional drinking-water-treatment plant, Sci. Total Environ. 329 (2004) 99–113. https://doi.org/10.1016/j.scitotenv.2004.03.015.
[5] M. Bilal, S.S. Ashraf, D. Barceló, H.M.N. Iqbal, Biocatalytic degradation/redefining "removal" fate of pharmaceutically active compounds and antibiotics in the aquatic environment, Sci. Total Environ. 691 (2019) 1190–1211. https://doi.org/10.1016/j.scitotenv.2019.07.224.
[6] B. Varga, V. Somogyi, M. Meiczinger, N. Kováts, E. Domokos, Enzymatic treatment and subsequent toxicity of organic micropollutants using oxidoreductases - A review, (2019). https://pubag.nal.usda.gov/catalog/6347190 (accessed September 16, 2019).
[7] J.D. Cui, S.R. Jia, Optimization protocols and improved strategies of cross-linked enzyme aggregates technology: current development and future challenges, Crit. Rev. Biotechnol. 35 (2015) 15–28. https://doi.org/10.3109/07388551.2013.795516.
[8] O. Barbosa, R. Torres, C. Ortiz, Á. Berenguer-Murcia, R.C. Rodrigues, R. Fernandez-Lafuente, Heterofunctional Supports in Enzyme Immobilization: From Traditional Immobilization Protocols to Opportunities in Tuning Enzyme Properties, Biomacromolecules. 14 (2013) 2433–2462. https://doi.org/10.1021/bm400762h.
[9] J. Boudrant, J.M. Woodley, R. Fernandez-Lafuente, Parameters necessary to define an immobilized enzyme preparation, Process Biochem. (2019). https://doi.org/10.1016/j.procbio.2019.11.026.
[10] J.J. Virgen-Ortíz, S.G. Pedrero, L. Fernandez-Lopez, N. Lopez-Carrobles, B.C. Gorines, C. Otero, R. Fernandez-Lafuente, Desorption of Lipases Immobilized on Octyl-Agarose Beads and Coated with Ionic Polymers after Thermal Inactivation. Stronger Adsorption of Polymers/Unfolded Protein Composites, Molecules. 22 (2017) 91. https://doi.org/10.3390/molecules22010091.
[11] M.C.P. Gonçalves, T.G. Kieckbusch, R.F. Perna, J.T. Fujimoto, S.A.V. Morales, J.P. Romanelli, Trends on enzyme immobilization researches based on bibliometric analysis, Process Biochem. 76 (2019) 95–110. https://doi.org/10.1016/j.procbio.2018.09.016.
[12] N.R. Mohamad, N.H.C. Marzuki, N.A. Buang, F. Huyop, R.A. Wahab, An overview of technologies for immobilization of enzymes and surface analysis techniques for immobilized enzymes, Biotechnol. Biotechnol. Equip. 29 (2015) 205–220. https://doi.org/10.1080/13102818.2015.1008192.
[13] P. Laveille, A. Falcimaigne, F. Chamouleau, G. Renard, J. Drone, F. Fajula, S. Pulvin, D. Thomas, C. Bailly, A. Galarneau, Hemoglobin immobilized on mesoporous silica as effective material for the removal of polycyclic aromatic hydrocarbons pollutants from water, New J. Chem. 34 (2010) 2153–2165. https://doi.org/10.1039/C0NJ00161A.
[14] P. Laveille, L.T. Phuoc, J. Drone, F. Fajula, G. Renard, A. Galarneau, Oxidation reactions using air as oxidant thanks to silica nanoreactors containing GOx/peroxidases bienzymatic systems, Catal. Today. 157 (2010) 94–100. https://doi.org/10.1016/j.cattod.2010.02.065.
[15] R. Cazelles, J. Drone, F. Fajula, O. Ersen, S. Moldovan, A. Galarneau, Reduction of CO 2 to methanol by a polyenzymatic system encapsulated in phospholipids–silica nanocapsules, New J. Chem. 37 (2013) 3721–3730. https://doi.org/10.1039/C3NJ00688C.

[16] A. Galarneau, M. Mureseanu, S. Atger, G. Renard, F. Fajula, Immobilization of lipase on silicas. Relevance of textural and interfacial properties on activity and selectivity, New J. Chem. 30 (2006) 562–571. https://doi.org/10.1039/B517104K.
[17] M. Mureseanu, N. Cioatera, I. Trandafir, I. Georgescu, F. Fajula, A. Galarneau, Selective Cu2+ adsorption and recovery from contaminated water using mesoporous hybrid silica bio-adsorbents, Microporous Mesoporous Mater. 146 (2011) 141–150. https://doi.org/10.1016/j.micromeso.2011.04.026.
[18] M. Hartmann, D. Jung, Biocatalysis with enzymes immobilized on mesoporous hosts : the status quo and future trends, J. Mater. Chem. 20 (2010) 844–857. https://doi.org/10.1039/B907869J.
[19] M. de Cazes, M.-P. Belleville, E. Petit, M. Llorca, S. Rodríguez-Mozaz, J. de Gunzburg, D. Barceló, J. Sanchez-Marcano, Design and optimization of an enzymatic membrane reactor for tetracycline degradation, Catal. Today. 236 (2014) 146–152. https://doi.org/10.1016/j.cattod.2014.02.051.
[20] M. de Cazes, M.-P. Belleville, M. Mougel, H.Kellner, J. Sanchez-Marcano, Characterization of laccase-grafted ceramic membranes for pharmaceuticals degradation, J. Membr. Sci. 476 (2015) 384–393. https://doi.org/10.1016/j.memsci.2014.11.044
[21] M. Taheran, M. Naghdi, S.K. Brar, E.J. Knystautas, M. Verma, R.Y. Surampalli, Covalent Immobilization of Laccase onto Nanofibrous Membrane for Degradation of Pharmaceutical Residues in Water, ACS Sustain. Chem. Eng. 5 (2017) 10430–10438. https://doi.org/10.1021/acssuschemeng.7b02465.
[22] L. Shi, F. Ma, Y. Han, X. Zhang, H. Yu, Removal of sulfonamide antibiotics by oriented immobilized laccase on Fe3O4 nanoparticles with natural mediators, J. Hazard. Mater. 279 (2014) 203–211. https://doi.org/10.1016/j.jhazmat.2014.06.070.
[23] A.A. Kadam, J. Jang, D.S. Lee, Supermagnetically Tuned Halloysite Nanotubes Functionalized with Aminosilane for Covalent Laccase Immobilization, ACS Appl. Mater. Interfaces. 9 (2017) 15492–15501. https://doi.org/10.1021/acsami.7b02531.
[24] X. Wen, Z. Zeng, C. Du, D. Huang, G. Zeng, R. Xiao, C. Lai, P. Xu, C. Zhang, J. Wan, L. Hu, L. Yin, C. Zhou, R. Deng, Immobilized laccase on bentonite-derived mesoporous materials for removal of tetracycline, Chemosphere. 222 (2019) 865–871. https://doi.org/10.1016/j.chemosphere.2019.02.020.
[25] J. Yang, Y. Lin, X. Yang, T.B. Ng, X. Ye, J. Lin, Degradation of tetracycline by immobilized laccase and the proposed transformation pathway, J. Hazard. Mater. 322 (2017) 525–531. https://doi.org/10.1016/j.jhazmat.2016.10.019.
[26] R. Abejon, M.P. Belleville, J. Sanchez-Marcano, Design, economic evaluation and optimization of enzymatic membrane reactors for antibiotics degradation in wastewaters, Sep. Purif. Technol. 156 (2015) 183–199. https://doi.org/10.1016/j.seppur.2015.09.072.
[27] R. Abejon, M. De Cazes, M.P. Belleville, J. Sanchez-Marcano, Large-scale enzymatic membrane reactors for tetracycline degradation in WWTP effluents, Water Res. 73 (2015) 118–131. https://doi.org/10.1016/j.watres.2015.01.012.
[28] A. Galarneau, A. Sachse, B. Said, C.-H. Pelisson, P. Boscaro, N. Brun, L. Courtheoux, N. Olivi-Tran, B. Coasne, F. Fajula, Hierarchical porous silica monoliths: A novel class of microreactors for process intensification in catalysis and adsorption, Comptes Rendus Chim. 19 (2016) 231–247. https://doi.org/10.1016/j.crci.2015.05.017.

[29] T. Westermann, T. Melin, Flow-through catalytic membrane reactors—Principles and applications, Chem. Eng. Process. Process Intensif. 48 (2009) 17–28. https://doi.org/10.1016/j.cep.2008.07.001.
[30] G. Puy, R. Roux, C. Demesmay, J.-L. Rocca, J. Iapichella, A. Galarneau, D. Brunel, Influence of the hydrothermal treatment on the chromatographic properties of monolithic silica capillaries for nano-liquid chromatography or capillary electrochromatography, J. Chromatogr. A. 1160 (2007) 150–159. https://doi.org/10.1016/j.chroma.2007.05.019.
[31] François Fajula, Anne Galarneau, Combining Phase Separation with Pseudomorphic Transformation for the Control of the Pore Architecture of Functional Materials: A Review, Pet. Chem. 59 (2019) 761–769. https://doi.org/10.1134/S0965544119080061.
[32] A. Sachse, V. Hulea, A. Finiels, B. Coq, F. Fajula, A. Galarneau, Alumina-grafted macro-/mesoporous silica monoliths as continuous flow microreactors for the Diels–Alder reaction, J. Catal. 287 (2012) 62–67. https://doi.org/10.1016/j.jcat.2011.12.003.
[33] H. Wang, Y. Jiang, L. Zhou, Y. He, J. Gao, Immobilization of penicillin G acylase on macrocellular heterogeneous silica-based monoliths, J. Mol. Catal. B Enzym. 96 (2013) 1–5. https://doi.org/10.1016/j.molcatb.2013.06.005.
[34] A. George, G.A. Radhakrishnan, K.T. Joseph, Grafting of Acrylonitrile onto Gelatin in Zinc Chloride Medium, J. Macromol. Sci. Part - Chem. 21 (1984) 179–191. https://doi.org/10.1080/00222338408056547.
[35] S.B. Ameur, C. Luminiţa Gîjiu, M.-P. Belleville, J. Sanchez, D. Paolucci-Jeanjean, Development of a multichannel monolith large-scale enzymatic membrane and application in an immobilized enzymatic membrane reactor, J. Membr. Sci. 455 (2014) 330–340. https://doi.org/10.1016/j.memsci.2013.12.026.
[36] W. Yao, Y. Li, N. Chen, Analytic solutions of the interstitial fluid flow models, J. Hydrodyn. Ser B. 25 (2013) 683–694. https://doi.org/10.1016/S1001-6058(13)60413-8.
[37] S.I. Vasin, A.N. Filippov, Permeability of complex porous media, Colloid J. 71 (2009) 31–45. https://doi.org/10.1134/S1061933X09010049.
[38] J.-L. Auriault, On the Domain of Validity of Brinkman's Equation, Transp. Porous Media. 79 (2009) 215–223. https://doi.org/10.1007/s11242-008-9308-7.
[39] M. Younas, S.D. Bocquet, J. Sanchez, Extraction of aroma compounds in a HFMC: Dynamic modelling and simulation, J. Membr. Sci. 323 (2008) 386–394. https://doi.org/10.1016/j.memsci.2008.06.045.
[40] A. Ciemięga, K. Maresz, J.J. Malinowski, J. Mrowiec-Białoń, Continuous-Flow Monolithic Silica Microreactors with Arenesulphonic Acid Groups: Structure–Catalytic Activity Relationships, Catalysts. 7 (2017) 255. https://doi.org/10.3390/catal7090255.
[41] A. Kumar, G.D. Park, S.K.S. Patel, S. Kondaveeti, S. Otari, M.Z. Anwar, V.C. Kalia, Y. Singh, S.C. Kim, B.-K. Cho, J.-H. Sohn, D.R. Kim, Y.C. Kang, J.-K. Lee, SiO2 microparticles with carbon nanotube-derived mesopores as an efficient support for enzyme immobilization, Chem. Eng. J. 359 (2019) 1252–1264. https://doi.org/10.1016/j.cej.2018.11.052.
[42] M. Llorca, S. Rodríguez-Mozaz, O. Couillerot, K. Panigoni, J. de Gunzburg, S. Bayer, R. Czaja, D. Barceló, Identification of new transformation products during enzymatic treatment of tetracycline and erythromycin antibiotics at laboratory scale by an on-line turbulent flow liquid-chromatography coupled to a high resolution mass spectrometer LTQ-orbitrap, Chemosphere, 119 (2015), 90-98. https://doi.org/10.1016/j.chemosphere.2014.05.072

[43] J. Yang, Y. Lin, X. Yang, T. B., Ng, X. Ye, J. Lin, Degradation of tetracycline by immobilized laccase and the proposed transformation pathway, J. Hazard. Mater.322 (2017) 525-531.
http://dx.doi.org/10.1016/j.jhazmat.2016.10.019